

## Special Issue: Bio-based Packaging

Guest Editors: José M. Lagarón, Amparo López-Rubio, and María José Fabra  
Institute of Agrochemistry and Food Technology of the Spanish Council for Scientific Research

### EDITORIAL

#### Bio-based Packaging

J. M. Lagarón, A. López-Rubio and M. J. Fabra, *J. Appl. Polym. Sci.* 2015,  
DOI: 10.1002/app.42971

### REVIEWS

#### Active edible films: Current state and future trends

C. Mellinas, A. Valdés, M. Ramos, N. Burgos, M. D. C. Garrigós and A. Jiménez,  
*J. Appl. Polym. Sci.* 2015, DOI: 10.1002/app.42631

#### Vegetal fiber-based biocomposites: Which stakes for food packaging applications?

M.-A. Berthet, H. Angellier-Coussy, V. Guillard and N. Gontard, *J. Appl. Polym. Sci.* 2015, DOI: 10.1002/app.42528

#### Enzymatic-assisted extraction and modification of lignocellulosic plant polysaccharides for packaging applications

A. Martínez-Abad, A. C. Ruthes and F. Vilaplana, *J. Appl. Polym. Sci.* 2015, DOI: 10.1002/app.42523

### RESEARCH ARTICLES

#### Combining polyhydroxyalkanoates with nanokeratin to develop novel biopackaging structures

M. J. Fabra, P. Pardo, M. Martínez-Sanz, A. Lopez-Rubio and J. M. Lagarón, *J. Appl. Polym. Sci.* 2015, DOI: 10.1002/app.42695

#### Production of bacterial nanobiocomposites of polyhydroxyalkanoates derived from waste and bacterial nanocellulose by the electrospinning enabling melt compounding method

M. Martínez-Sanz, A. Lopez-Rubio, M. Villano, C. S. S. Oliveira, M. Majone, M. Reis and J. M. Lagarón, *J. Appl. Polym. Sci.* 2015,  
DOI: 10.1002/app.42486

#### Bio-based multilayer barrier films by extrusion, dispersion coating and atomic layer deposition

J. Vartiainen, Y. Shen, T. Kaljunen, T. Malm, M. Vähä-Nissi, M. Putkonen and A. Harlin, *J. Appl. Polym. Sci.* 2015,  
DOI: 10.1002/app.42260

#### Film blowing of PHBV blends and PHBV-based multilayers for the production of biodegradable packages

M. Cunha, B. Fernandes, J. A. Covas, A. A. Vicente and L. Hilliou, *J. Appl. Polym. Sci.* 2015, DOI: 10.1002/app.42165

#### On the use of tris(nonylphenyl) phosphite as a chain extender in melt-blended poly(hydroxybutyrate-co-hydroxyvalerate)/clay nanocomposites: Morphology, thermal stability, and mechanical properties

J. González-Ausejo, E. Sánchez-Safont, J. Gámez-Pérez and L. Cabedo, *J. Appl. Polym. Sci.* 2015, DOI: 10.1002/app.42390

#### Characterization of polyhydroxyalkanoate blends incorporating unpurified biosustainably produced poly(3-hydroxybutyrate-co-3-hydroxyvalerate)

A. Martínez-Abad, L. Cabedo, C. S. S. Oliveira, L. Hilliou, M. Reis and J. M. Lagarón, *J. Appl. Polym. Sci.* 2015,  
DOI: 10.1002/app.42633

#### Modification of poly(3-hydroxybutyrate-co-3-hydroxyvalerate) properties by reactive blending with a monoterpene derivative

L. Pilon and C. Kelly, *J. Appl. Polym. Sci.* 2015, DOI: 10.1002/app.42588

#### Poly(3-hydroxybutyrate-co-3-hydroxyvalerate) films for food packaging: Physical-chemical and structural stability under food contact conditions

V. Chea, H. Angellier-Coussy, S. Peyron, D. Kemmer and N. Gontard, *J. Appl. Polym. Sci.* 2015, DOI: 10.1002/app.41850



## Special Issue: Bio-based Packaging

Guest Editors: José M. Lagarón, Amparo López-Rubio, and María José Fabra  
Institute of Agrochemistry and Food Technology of the Spanish Council for Scientific Research

Impact of fermentation residues on the thermal, structural, and rheological properties of polyhydroxy(butyrate-co-valerate) produced from cheese whey and olive oil mill wastewater  
L. Hilliou, D. Machado, C. S. S. Oliveira, A. R. Gouveia, M. A. M. Reis, S. Campanari, M. Villano and M. Majone, *J. Appl. Polym. Sci.* 2015, DOI: [10.1002/app.42818](https://doi.org/10.1002/app.42818)

Synergistic effect of lactic acid oligomers and laminar graphene sheets on the barrier properties of polylactide nanocomposites obtained by the in situ polymerization pre-incorporation method

J. Ambrosio-Martín, A. López-Rubio, M. J. Fabra, M. A. López-Manchado, A. Sorrentino, G. Gorrasi and J. M. Lagarón, *J. Appl. Polym. Sci.* 2015, DOI: [10.1002/app.42661](https://doi.org/10.1002/app.42661)

Antibacterial poly(lactic acid) (PLA) films grafted with electrospun PLA/allyl isothiocyanate fibers for food packaging

H. H. Kara, F. Xiao, M. Sarker, T. Z. Jin, A. M. M. Sousa, C.-K. Liu, P. M. Tomasula and L. Liu, *J. Appl. Polym. Sci.* 2015, DOI: [10.1002/app.42475](https://doi.org/10.1002/app.42475)

Poly(L-lactide)/ZnO nanocomposites as efficient UV-shielding coatings for packaging applications

E. Lizundia, L. Ruiz-Rubio, J. L. Vilas and L. M. León, *J. Appl. Polym. Sci.* 2015, DOI: [10.1002/app.42426](https://doi.org/10.1002/app.42426)

Effect of electron beam irradiation on the properties of polylactic acid/montmorillonite nanocomposites for food packaging applications

M. Salvatore, A. Marra, D. Duraccio, S. Shayanfar, S. D. Pillai, S. Cimmino and C. Silvestre, *J. Appl. Polym. Sci.* 2015, DOI: [10.1002/app.42219](https://doi.org/10.1002/app.42219)

Preparation and characterization of linear and star-shaped poly L-lactide blends

M. B. Khajeheian and A. Rosling, *J. Appl. Polym. Sci.* 2015, DOI: [10.1002/app.42231](https://doi.org/10.1002/app.42231)

Mechanical properties of biodegradable polylactide/poly(ether-block-amide)/thermoplastic starch blends: Effect of the crosslinking of starch

L. Zhou, G. Zhao and W. Jiang, *J. Appl. Polym. Sci.* 2015, DOI: [10.1002/app.42297](https://doi.org/10.1002/app.42297)

Interaction and quantification of thymol in active PLA-based materials containing natural fibers

I. S. M. A. Tawakkal, M. J. Cran and S. W. Bigger, *J. Appl. Polym. Sci.* 2015, DOI: [10.1002/app.42160](https://doi.org/10.1002/app.42160)

Graphene-modified poly(lactic acid) for packaging: Material formulation, processing, and performance

M. Barletta, M. Puopolo, V. Tagliaferri and S. Vesco, *J. Appl. Polym. Sci.* 2015, DOI: [10.1002/app.42252](https://doi.org/10.1002/app.42252)

Edible films based on chia flour: Development and characterization

M. Dick, C. H. Pagno, T. M. H. Costa, A. Gomaa, M. Subirade, A. De O. Rios and S. H. Flóres, *J. Appl. Polym. Sci.* 2015, DOI: [10.1002/app.42455](https://doi.org/10.1002/app.42455)

Influence of citric acid on the properties and stability of starch-polycaprolactone based films

R. Ortega-Toro, S. Collazo-Bigliardi, P. Talens and A. Chiralt, *J. Appl. Polym. Sci.* 2015, DOI: [10.1002/app.42220](https://doi.org/10.1002/app.42220)

Bionanocomposites based on polysaccharides and fibrous clays for packaging applications

A. C. S. Alcântara, M. Darder, P. Aranda, A. Ayral and E. Ruiz-Hitzky, *J. Appl. Polym. Sci.* 2015, DOI: [10.1002/app.42362](https://doi.org/10.1002/app.42362)

Hybrid carrageenan-based formulations for edible film preparation: Benchmarking with kappa carrageenan

F. D. S. Larotonda, M. D. Torres, M. P. Gonçalves, A. M. Sereno and L. Hilliou, *J. Appl. Polym. Sci.* 2015, DOI: [10.1002/app.42263](https://doi.org/10.1002/app.42263)



Special Issue: Bio-based Packaging

Guest Editors: José M. Lagarón, Amparo López-Rubio, and María José Fabra  
Institute of Agrochemistry and Food Technology of the Spanish Council for Scientific Research

Structural and mechanical properties of clay nanocomposite foams based on cellulose for the food packaging industry

S. Ahmadzadeh, J. Keramat, A. Nasirpour, N. Hamdami, T. Behzad, L. Aranda, M. Vilasi and S. Desobry, *J. Appl. Polym. Sci.* 2015, DOI: [10.1002/app.42079](https://doi.org/10.1002/app.42079)

Mechanically strong nanocomposite films based on highly filled carboxymethyl cellulose with graphene oxide

M. El Achaby, N. El Miri, A. Snik, M. Zahouily, K. Abdelouahdi, A. Fihri, A. Barakat and A. Solhy, *J. Appl. Polym. Sci.* 2015, DOI: [10.1002/app.42356](https://doi.org/10.1002/app.42356)

Production and characterization of microfibrillated cellulose-reinforced thermoplastic starch composites

L. Lendvai, J. Karger-Kocsis, Á. Kmetty and S. X. Drakopoulos, *J. Appl. Polym. Sci.* 2015, DOI: [10.1002/app.42397](https://doi.org/10.1002/app.42397)

Development of bioplastics based on agricultural side-stream products: Film extrusion of *Crambe abyssinica*/wheat gluten blends for packaging purposes

H. Rasel, T. Johansson, M. Gällstedt, W. Newson, E. Johansson and M. Hedenqvist, *J. Appl. Polym. Sci.* 2015, DOI: [10.1002/app.42442](https://doi.org/10.1002/app.42442)

Influence of plasticizers on the mechanical and barrier properties of cast biopolymer films

V. Jost and C. Stramm, *J. Appl. Polym. Sci.* 2015, DOI: [10.1002/app.42513](https://doi.org/10.1002/app.42513)

The effect of oxidized ferulic acid on physicochemical properties of bitter vetch (*Vicia ervilia*) protein-based films

A. Arabestani, M. Kadivar, M. Shahedi, S. A. H. Goli and R. Porta, *J. Appl. Polym. Sci.* 2015, DOI: [10.1002/app.42894](https://doi.org/10.1002/app.42894)

Effect of hydrochloric acid on the properties of biodegradable packaging materials of carboxymethylcellulose/poly(vinyl alcohol) blends

M. D. H. Rashid, M. D. S. Rahaman, S. E. Kabir and M. A. Khan, *J. Appl. Polym. Sci.* 2015, DOI: [10.1002/app.42870](https://doi.org/10.1002/app.42870)



## Interaction and quantification of thymol in active PLA-based materials containing natural fibers

Intan S. M. A. Tawakkal,<sup>1</sup> Marlene J. Cran,<sup>2</sup> Stephen W. Bigger<sup>1</sup>

<sup>1</sup>College of Engineering and Science, Victoria University, Melbourne 8001, Australia

<sup>2</sup>Institute for Sustainability and Innovation, Victoria University, Melbourne 8001, Australia

Correspondence to: M. J. Cran (E-mail: marlene.cran@vu.edu.au)

**ABSTRACT:** The quantification of thymol, a commercial essential oil extract that is an antimicrobial (AM) agent, in poly(lactic acid) (PLA) and PLA/kenaf composites was investigated to explore the potential of these systems as AM food-packaging materials. Neat PLA and PLA/kenaf composites containing thymol (5–10 wt %) were prepared *via* melt blending and compression molding. The quantification of the thymol content in PLA and PLA/kenaf composites after processing as well as the interactions between the PLA matrix, kenaf fibers and the AM agent were investigated. The PLA/kenaf composites in the range of 10 to 40 wt % fiber content retained less thymol upon processing than PLA alone and the composites containing the highest fiber loadings demonstrated the lowest thymol retention. The observed losses were attributed to the higher mechanical shear that exists during the mixing process as well as the creation of voids in the composites that facilitate the release of thymol from the system. © 2015 Wiley Periodicals, Inc. *J. Appl. Polym. Sci.* 2016, 133, 42160.

**KEYWORDS:** biopolymers and renewable polymers; composites; fibers; packaging; thermal properties

Received 16 December 2014; accepted 5 March 2015

DOI: 10.1002/app.42160

### INTRODUCTION

The utilization of biocomposites for active food packaging is currently under investigation with a major purpose being to reduce environmental pollution as well as recover biodegradable polymers.<sup>1–3</sup> Nowadays, renewable polymers such as PLA that are derived and synthesized from plant materials are widely used for films and coatings as well as matrices for incorporating naturally sourced additives such as antimicrobial (AM) agents that prolong the shelf life of packaged food products.<sup>4–7</sup> Several additives have been incorporated directly into polymers including organic acids, enzymes, bacteriocins, chelators and a range of plant extracts.<sup>8–11</sup>

For food-packaging applications, the concept of AM agent migration is used to provide continuous AM activity to food products. This can be achieved by using volatile additives derived from plant extracts (e.g., essential oils) whereby these natural agents are considered to be much safer than synthetically derived chemical agents.<sup>12</sup> Thymol and carvacrol which are the major constituents of thyme essential oil can act as antioxidants and AM agents. These compounds are amongst the most currently studied natural additives that can be incorporated into packaging materials.<sup>13–17</sup> However, essential oils have low thermal stability and high volatility and so their exposure to high temperature, shearing and pressure during processing (e.g.,

extrusion, injection and blown molding) often results in their loss from the matrix and consequently a reduction in the AM activity of the system.<sup>15</sup> For instance, extruded PLA demonstrated a loss of thymol with lower inhibition of *Listeria monocytogenes*.<sup>11</sup> Furthermore, PLA has a relatively lower melting temperature than many commercial food-packaging materials such as poly(ethylene terephthalate). Nevertheless, the processing temperature of PLA using an extruder is normally greater than 150°C and this is crucial to ensure optimal melt viscosity as well as the complete melting of the crystalline phase in the matrix during extrusion.<sup>18</sup> Such conditions enable the AM agent to be evenly distributed in the amorphous regions of the polymeric material and thus regulate a slow release of the agent from the film.<sup>19</sup>

Plasticizers and fillers such as polyethylene glycol (PEG), natural fibers and nanofillers are used to facilitate the controlled release and to increase the activity of AM agents. Recent studies by Ramos *et al.*<sup>20</sup> reported an increment in the thermal stability of the essential oil thymol upon processing due to the incorporation of nanoclay (e.g., montmorillonite) into active PLA films where the nanoclay was incorporated to control the thymol release in the active films. Liu *et al.*<sup>21</sup> reported that the incorporation of plasticizers during the extrusion process lowered the temperature profile during the manufacturing of AM films.

In that study, PLA/Nisaplin films showed no AM activity whereas PLA blended with the lactide dimer of PLA and PLA plasticized with glycerol triacetate (GTA) that were used to create membranes containing Nisaplin each prevented the growth of *L. monocytogenes* in (BHI) broth. Praprudivongs and Sombatsompop<sup>22</sup> found that a higher loading of wood flour (10 wt %) resulted in facilitating the release of more triclosan onto a PLA composite surface due to the hydrophilic nature of the wood flour causing water molecules to be absorbed by the surface of the composite. Similar findings were reported by Woraprayote *et al.*<sup>23</sup> where sawdust particles helped to embed pediocin into coated PLA composites and significantly inhibited the growth of *L. monocytogenes* in agar media and sliced pork mince. Nevertheless, in these studies, there is little information on the quantification of AM agents after the processing of the active PLA-based materials containing natural fibers.

It is clear that more research needs to be conducted to investigate the quantification of AM agents when high temperature, shear and pressure are applied during processing. The release profile and AM inhibition activity in order to produce efficient active films or materials also requires further investigation along with the possible interaction of the AM agent with other additives in the matrix. To date, it appears that no study in the literature has systematically addressed the quantification of thymol or other essential oil AM agents after plastic thermal processing for PLA-based materials containing natural fibers. In the current study, a natural fibrous substance, namely kenaf fiber (*Hibiscus cannabinus L.*), is of interest as a reinforcing filler for PLA-based composites. The composite material is expected to be advantageous when compared to many synthetic composite materials due to the renewability of the raw materials from which it is comprised and its propensity to be environmentally friendly.<sup>2,23,24</sup> Moreover, the incorporation of the natural fibers as a filler in the biopolymer can also improve its mechanical properties, reduce abrasion resistance during processing, promote good compatibility and enhance biodegradability.<sup>25,26</sup> Tawakkal *et al.*<sup>7</sup> reported that the PLA/kenaf composites demonstrated improved mechanical properties such as tensile strength and stiffness compared with commercial PLA due to the reinforcement of the kenaf fibers in the PLA matrix. However, the increased stiffness and hence less flexibility means that these materials are perhaps more suitable to be developed as rigid food-packaging materials.

The objective of this study is to quantitatively investigate the retention of thymol incorporated into PLA and PLA/kenaf composite films during processing as well as the thermal release kinetics of thymol from these materials. These parameters are of importance in order to understand the interactions amongst the matrix, natural fibers and AM agents in the films and the ability of the films to initiate and maintain effective AM activity.

## EXPERIMENTAL

### Materials

Poly(lactic acid) (7001D Ingeo<sup>TM</sup>; specific gravity 1.24; melt flow index (MFI) 6 g/10 min at 210°C and 2.16 kg; melting temperature range 145–160°C) was obtained from NatureWorks LLC. Mechanically separated kenaf fiber (bast) was purchased

from Ecofibre Industries, Australia. The thymol (T0501, purity of 99.5%) was purchased from Sigma Aldrich Pty. Ltd., Australia. Sodium hydroxide and acetic acid were purchased from Merck Chemicals, Australia. Un-denatured ethanol was purchased from Chem-Supply Pty Ltd., Australia. Isooctane (2,2,4-trimethylpentane, 36006) was purchased from Sigma Aldrich, Australia.

### Preparation of Active PLA/Kenaf/Thymol Composites

The kenaf fiber surface treatment was performed by immersing fibers in 5% w/v sodium hydroxide (NaOH) for 2 h at room temperature. Acetic acid was used to adjust the pH (until neutralized) during the process of washing and rinsing the fibers with distilled water. Treated kenaf (TK) fibers were filtered from the solution, washed, and later dried overnight in an air oven at 105°C. The dried fibers were then ground and sieved using a 300–500 µm aperture sieve. The aspect ratio (L/D) of the kenaf fibers was approximately 9 with an average length of 920 µm and an average diameter of 104 µm. The preparation of untreated kenaf (UK) and TK doped with thymol was performed by immersing 20 g of fibers in 800 mL of 10–25% v/w thymol/ethanol solution and stirring for 1–2 h. The doped fibers were then filtered from the solution and dried overnight in a laminar flow cabinet in order to evaporate the remaining ethanol. The micrograph images of TK and TK doped with 25 wt % thymol can be seen in Figure 1. These show that the doping of the TK was successful as a smooth fiber surface is observed on the doped TK sample. Prior to mixing, the PLA resin was dried in an oven at 60°C overnight before blending with kenaf (undoped and doped with thymol) at various concentrations in the range zero to 40 wt %.

To produce active PLA as well as PLA/kenaf films, the PLA, UK or TK fibers (zero to 40 wt %) or thymol were compounded using an internal mixer (Haake PolyLab OS, Germany) at 50 rpm and at a processing temperature of 155°C for 8–10 min. The samples were prepared by using a laboratory press (L0003, IDM Instrument Pty. Ltd., Australia). The PLA and composites were preheated at 150°C for 2 min and pressed at the same temperature for 3 min under a pressure of 50 kN before quench cooling to 30°C under pressure. The average thickness of the heat pressed PLA and PLA/kenaf films incorporated with thymol were  $0.19 \pm 0.03$  and  $0.25 \pm 0.05$  respectively. A hand-held micrometer (Hahn & Kolb, Stuttgart, Germany) was used for measuring the film thickness.

### Infrared Analyses

The infrared spectral analysis of PLA and PLA/kenaf composite film samples was performed using a Shimadzu IR Prestige Fourier transform infrared (FTIR) spectrophotometer and utilizing the attenuated total reflectance (ATR) technique. For thymol and kenaf fiber samples, a small portion of thymol or kenaf fiber powder was mixed in an agate mortar and pestle with a few drops of paraffin oil. The sample was then applied to a KBr disc and its FTIR spectrum recorded. All spectra were recorded in absorbance mode in the range of 550–4000  $\text{cm}^{-1}$  with a resolution of 4  $\text{cm}^{-1}$  and with 32 scans recorded at every point using Happ-Genzel apodization. Ten scans were performed for each acquisition.

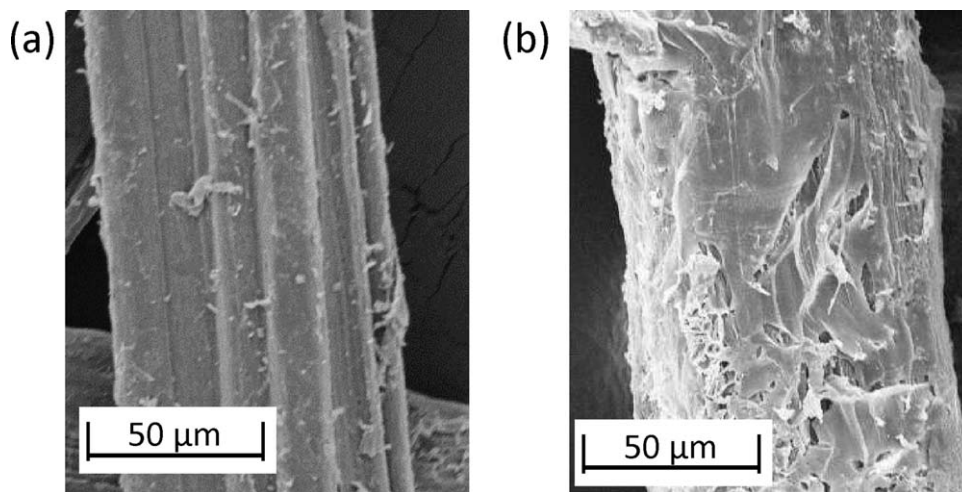


**Figure 1.** Scanning electron micrographs of: (a) TK fiber at 500 $\times$  magnification and (b) TK fiber doped with 25 wt % thymol at 500 $\times$  magnification.

### Thermogravimetric Analyses

A Mettler Toledo (TGA/DSC 1 Star System) was used to undertake the thermogravimetric (TG) analyses. The weight percentage of thymol that was retained in the samples after processing was measured from the normalized weight loss curve and the derivative of the weight loss curve, the latter being used to identify the start and end points of the process. The PLA and PLA/kenaf composite samples containing thymol were heated from 30 to 500 $^{\circ}\text{C}$  at a heating rate of 5 $^{\circ}\text{C min}^{-1}$  and under a nitrogen atmosphere flow rate of 0.2 L  $\text{min}^{-1}$ .

### Thymol Quantification in PLA and PLA/Kenaf Composites

Reflux extraction followed by gas chromatography (GC) was used to analytically determine the weight percentage of thymol that was retained in the samples after processing. One gram of compressed sample was extracted at 100 $^{\circ}\text{C}$  for 2–5 h using 100 mL of isooctane or 95% ethanol. An aliquot of the solution was analyzed using GC. The conditions applied in the GC instrument were as follows: injected volume, 1.0  $\mu\text{L}$ ; initial column temperature, 80 $^{\circ}\text{C}$ ; heating rate, 5 $^{\circ}\text{C min}^{-1}$  up to 120 $^{\circ}\text{C}$ , held at this temperature for an additional 5 min; injector temperature, 250 $^{\circ}\text{C}$ ; FID detector temperature, 300 $^{\circ}\text{C}$ ; flow rate, 2 mL  $\text{min}^{-1}$ ; splitting; carrier gas, nitrogen. A standard curve for thymol was also prepared and the thymol content of the samples was calculated using this curve.

### Thymol Release Using TG Kinetic Analyses

The application of non-isothermal techniques for the determination of kinetic parameters of reaction measured by loss in weight has been long established.<sup>27</sup> In the current study, non-isothermal TG kinetic analyses of the release of thymol from PLA and PLA/kenaf composite samples were performed by a computer-based iterative numerical method using original software. The software was developed to execute an integral solution of the general kinetic equation pertaining to TG analysis:

$$g(\alpha) = (AEa/R\beta) \times p(x) \quad (1)$$

where  $\alpha$  is the degree of conversion at time  $t$  in the process,  $A$  is the Arrhenius A-factor,  $Ea$  is the apparent activation energy

for the process,  $R$  is the ideal gas constant and  $\beta$  is the heating rate. The function  $p(x)$  represents the integral:

$$p(x) = \int_x^{\infty} [\exp(-x)/x^2] dx \quad (2)$$

where  $x = Ea/RT$  and  $T$  is the absolute temperature. The data pertaining to the release of thymol were analyzed according to a 3D diffusional model<sup>28</sup> and an algorithm developed from the work of Dollimore *et al.*<sup>29</sup> was used to confirm that this model was the most appropriate one needed to fit the data. For a 3D diffusion model:

$$g(\alpha) = [1 - (1-\alpha)^{1/3}]^2 \quad (3)$$

All TGA profiles were analyzed up to 85% conversion with respect to the corresponding first step in the TG analysis profile in order to extract the apparent activation energy and Arrhenius A-Factor data.

### Morphology of Fibers and Composites

Scanning electron microscopy (SEM) was conducted to observe the morphology of TK, TK doped with thymol as well as that of the composites. The composite films were immersed in liquid nitrogen and then fractured in order to create a fracture surface of the films for observation. All micrographs were obtained using a JOEL NeoScope (JCM-5000) scanning electron microscope. Samples were coated with a thin layer of gold (6 nm) using a NeoCoater (MP19020NCTR) device under high vacuum and using an optimal accelerating voltage of 10 kV to avoid charging effects.

## RESULTS AND DISCUSSION

### Structural Properties

Figure 2 shows the FTIR spectra of the neat PLA, thymol and TK fibers. The absence of the O–H stretching band in the spectrum of the neat PLA confirms that this particular grade of PLA (7001D) is hydrophobic. The carbonyl ( $>\text{C}=\text{O}$ ) stretching peak at 1746  $\text{cm}^{-1}$  is due to the carbonyl group in the lactic acid ester moiety of PLA.<sup>30</sup> The deformational vibrations of C–H in the methyl group of PLA are also observed in the range

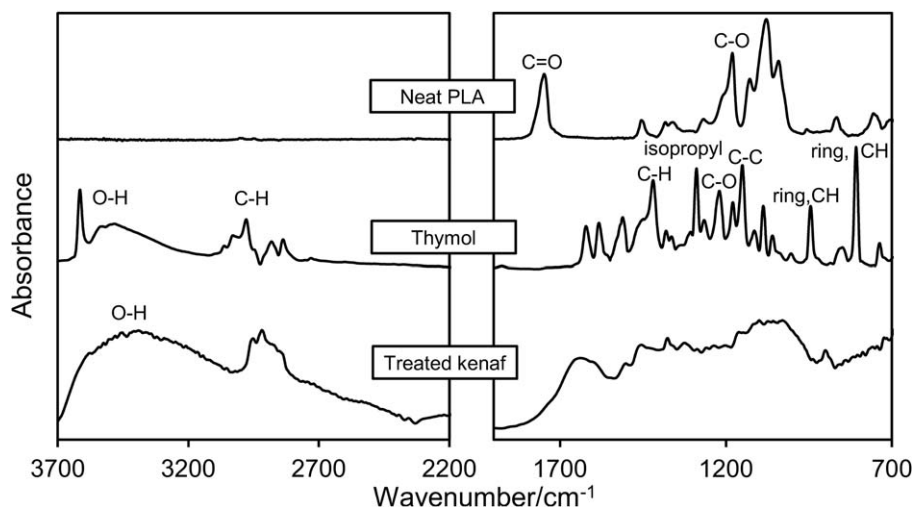


Figure 2. FTIR spectra of PLA, thymol and TK fiber.

of 1300 to 1500  $\text{cm}^{-1}$ .<sup>30</sup> The peak at 1180  $\text{cm}^{-1}$  is due to the stretching vibration of C—O—C and another asymmetric stretching vibration of C—O—C is observed in the range of 1150–1060  $\text{cm}^{-1}$ .<sup>31</sup>

The FTIR spectrum of thymol exhibits a number of major peaks as seen in Figure 2 and these are also tabulated in Table I along with the major peaks observed in the spectra of PLA and PLA/TK composites containing thymol. The following spectral features are apparent in Figure 2: a broad band due to the O—H hydroxyl group stretching vibration appears in the range of 3400–3500  $\text{cm}^{-1}$ ; the C—H methyl group stretching at 2945  $\text{cm}^{-1}$ ; a strong absorption due to the phenolic C—O stretching in the region at 1215  $\text{cm}^{-1}$ ; C—C stretching at 1419  $\text{cm}^{-1}$ ; and strong peaks due to isopropyl stretching and ring aromatic C—H bending at 1288  $\text{cm}^{-1}$  and 810  $\text{cm}^{-1}$  respectively.<sup>32</sup> Moreover, the FTIR spectrum of the TK fibers exhibits a broad O—H band at 3500–3400  $\text{cm}^{-1}$  with the expected absence of a sharp, carbonyl group absorption at approximately 1700  $\text{cm}^{-1}$ . This is due to the removal of ester groups in the hemicellulose during the alkali treatment of the surface of the kenaf fibers.<sup>33</sup> A similar observation was reported by Himmelsbach *et al.*<sup>34</sup> who found that the ester groups of hemicellulose or the ester linkage of the carboxylic group of ferulic and *p*-coumaric acids of lignin and/or hemicellulose disappeared in the spectrum of cellulose fibers.

From Table I, it can be noted that the spectra of the PLA and PLA/TK composites containing thymol are similar. This could be due to the high content of PLA present in the surface of the pressed films. Nevertheless, each of the PLA and PLA/TK composites containing 20 wt % thymol demonstrated a significant shift of O—H group absorptions that appear in the regions of approximately 3510  $\text{cm}^{-1}$  respectively as compared with the thymol spectrum. This suggests that the thymol interacts with the PLA and/or the TK fibers. Intermolecular hydrogen bonding is presumed to exist between thymol and TK as well as thymol and PLA. Furthermore, hydrogen bonding is likely to be present in the composite between the hydroxyl groups in the TK fibers and the terminal hydroxyl groups of PLA,<sup>35</sup> the carbonyl groups

of the ester linkages of PLA<sup>36</sup> as well as the thymol terminal hydroxyl group. The FTIR spectrum of the PLA/TK composite containing 20 wt % TK and 20 wt % thymol was similar to that of the PLA containing 20 wt % thymol (see Table I). A small but noticeable peak broadening of the hydroxyl group absorption was observed in the active PLA/TK composite compared to PLA containing 20 wt % thymol. This is attributable to the presence of the hydrophilic TK fibers in the composite [see Figure 3(a)].

Figure 3(b) shows the normalized carbonyl absorptions of neat PLA and PLA/TK composites containing 20 wt % thymol, where a slight hypsochromic shift in the carbonyl peak (at 1755  $\text{cm}^{-1}$ ) of the PLA is observed upon the addition of thymol to the PLA. A small shoulder on the peak is observed in the carbonyl group absorption at 1750  $\text{cm}^{-1}$  for PLA containing 20 wt % thymol and this shoulder becomes more pronounced with the presence of TK fibers in the film. The peak shift and presence of the peak shoulder support the notion of an intermolecular interaction existing between the PLA and thymol. A similar observation was made by Praprudivongs and Sombatsompop<sup>22</sup> who investigated the interaction between PLA, 10 wt % wood flour and 1.5 wt % triclosan by using FTIR. They reported that the incorporation of triclosan and wood flour into PLA broadened the carbonyl absorbance peak and caused carbonyl peak splitting at wavenumbers of 1753 and 1746  $\text{cm}^{-1}$ . The data listed in Table I suggest that overall the PLA/TK composite demonstrates similar spectral features to those of neat PLA. The hydroxyl group absorption at a wavenumber of *ca.* 3515  $\text{cm}^{-1}$  is possibly due to the low amount of fibers on the surface of the pressed film. These fibers are expected to create a surface roughness and may inhibit the resolution of the ATR technique compared to the case of PLA alone.

### Thermal Properties

Figure 4 shows the normalized weight loss as a function of temperature for PLA composites containing TK and 10 wt % thymol. The profiles typically show an initial step that occurs over the temperature range of *ca.* 90–300°C and corresponds to the degradation/release of thymol from the matrix.<sup>13</sup> The second,

**Table I.** Major Peaks of Thymol, PLA and PLA Containing Thymol and TK Fibers

Functional group	Thymol	PLA	PLA/thymol <sup>a</sup>	PLA/TK <sup>b</sup>	PLA/thymol/TK <sup>c</sup>	Notes
OH	3483.6	-	3510.9	3505.8	3514.5	Significant shift of thymol O—H band incorporated in composite; peak broadening with presence of TK
CH	2978.2	2951.2	2945.4	2951.2	2947.4	Significant shift of thymol C—H stretch when incorporated in PLA and PLA/TK
C=O	-	1747.6	1750.5	1747.6	1755.4	Small shift in C=O absorption across the active composites; peak broadening in active composites <i>cf.</i> neat PLA
Ring CH	945.2	-	947.1	-	947.1	Small shift of thymol ring C—H stretch when incorporated in PLA and PLA/TK
CH	2881.8	-	2875.9	-	2875.9	No significant shift
Ring	1622.2	-	1620.3	-	1618.4	No significant shift; weak peak
Ring	1581.7	-	1585.6	-	1585.6	No significant shift; weak peak
CC	1419.7	-	1423.5	-	1419.7	No significant shift; weak peak
CH or CC isopropyl	1288.5	-	1292.4	-	1292.4	No significant shift; weak peak
COC	-	1180.5	1180.5	1180.5	1182.5	No significant shift; peak broadening in composites <i>cf.</i> neat PLA
COC	-	1078.3	1082.1	1078.3	1084.1	No significant shift; peak broadening in composites <i>cf.</i> neat PLA
Ring CH	808.2	-	810.1	-	810.1	No significant shift

<sup>a</sup>thymol at 20 wt %; <sup>b</sup> TK fiber at 20 wt %; <sup>c</sup> PLA containing 20 wt % TK fiber and 20 wt % thymol

more pronounced step at 300–370°C corresponds to the degradation of the PLA that presumably occurs by thermal depolymerization and decomposition.<sup>37</sup> As the TK loading in the formulation is increased the level of char remaining in the system at elevated temperatures (*ca.* 390°C and above) is observed to increase accordingly.

The quantification of thymol in the PLA and PLA/TK composites can be calculated from the TG profile as in the work of Ramos *et al.*<sup>20</sup> who investigated the retention of thymol in a PLA matrix and found that there was some loss of this volatile AM agent during processing. An example of a detailed analysis of the TG profiles obtained in the current study is shown in Figure 5 that shows the first derivative with respect to temperature,  $dw/dT$ , of the TG weight loss profiles. The value of the initial temperature at which thymol is released,  $T_{rel}$ , decreases by *ca.* 3.8°C upon the addition of 40 wt % TK to the formulation (see Figure 5) suggesting that the addition of TK to the polymer facilitates the loss of thymol from the PLA matrix. Similarly, a smaller decrease of *ca.* 1.7°C in  $T_{rel}$  is also observed in the case where 10 wt % of TK is present in the formulation although this decrease may not be significant. These findings are also supported by the observation that the temperature at which the maximum rate of degradation of PLA occurs,  $T_{deg}$ , is lower in the case of the sample with the highest loading of fiber than in the case of PLA alone.

The values of  $T_{rel}$ ,  $T_{deg}$  and the percentage of char residue of the various formulations were determined from the complete TG analyses and these are summarized in Table II. Overall, it was found that the  $T_{rel}$  value of PLA/TK composites decreased with increasing TK fiber loading from 10% to 40 wt % over the temperature range of 149.9 to 144.0°C. Thus, it is clear from the results in Table II that the addition of TK to the formulation decreases the temperature at which thymol is released from the matrix at maximum rate and also decreases the temperature at which the maximum rate of degradation of the PLA occurs under the temperature ramp. The latter suggests that the addition of fiber destabilizes the polymer to some extent.<sup>38</sup> Moreover, the addition of 5–10 wt % thymol has no significant effect on the value of the  $T_{deg}$  of PLA and this finding is in agreement with the work of Ramos *et al.*<sup>20</sup> who investigated the TG properties of PLA containing 8 wt % thymol. Thus, the addition of thymol to the formulation has little effect on the thermal stability of the material as a whole whereas the addition of TK affects the thermal stability.

#### Quantification of Thymol

The effect of adding TK to the formulation on the quantification of thymol released from the matrix can be further explored by plotting the normalized  $T_{rel}$  values of PLA/kenaf composites containing 5 and 10 wt % thymol at various TK loadings in the range of zero to 40 wt % (see Figure 6). An almost linear



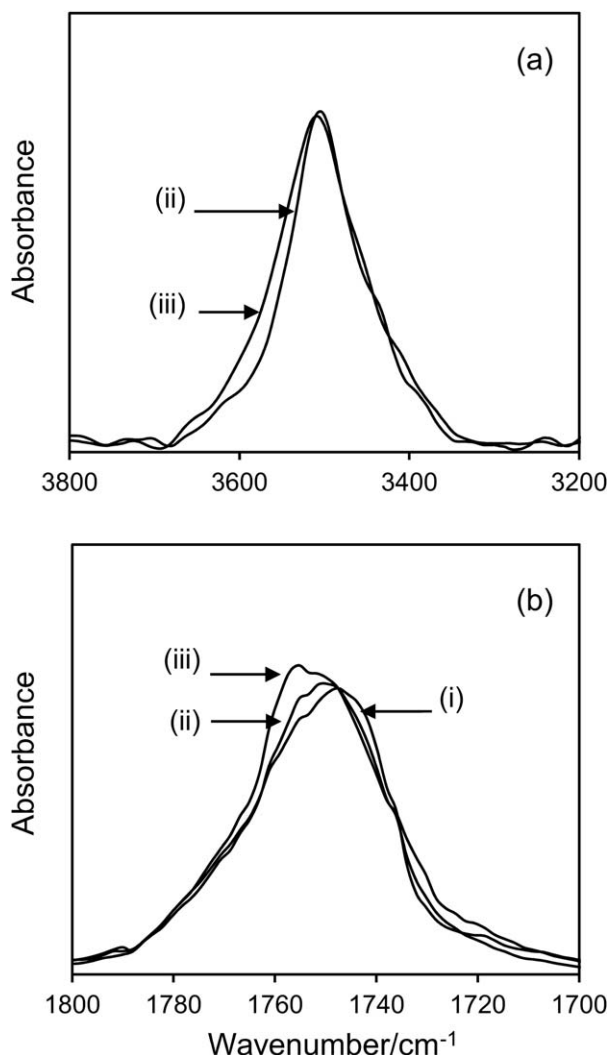


**Figure 3.** FTIR spectra showing: (a) hydroxyl group and (b) carbonyl group absorptions for: (i) neat PLA, (ii) PLA containing 20 wt % thymol, and (iii) PLA/TK fiber composite containing 20 wt % thymol.

reduction in the  $T_{rel}$  with the addition of TK fiber was observed at each of the concentrations of thymol for which the composite containing 40 wt % kenaf showed the lowest  $T_{rel}$  (see Figure 6 and Table II). This suggests that the presence of the less thermally stable fibers may also destabilize the PLA-thymol matrix. Moreover, no significant change was observed for the  $T_{rel}$  of PLA and PLA/TK composite formulations containing 5 and 10 wt % thymol.

The effect of fillers such as TK on the release of thymol from the polymer matrix has important implications particularly with regard to the loss of the active agent during processing. The TG analysis technique can be used to provide indirect confirmation of the presence of AM agents in the polymer matrix after thermal processing<sup>39</sup> and so to this end it was decided to utilize the technique to investigate the effect of the TK filler on the quantification of thymol in the PLA system following thermal processing. The results from the TG experiments were corrected for the inherent water content of the TK fibers and the analytical results were also verified by solid-liquid extraction and GC analysis.<sup>19</sup>

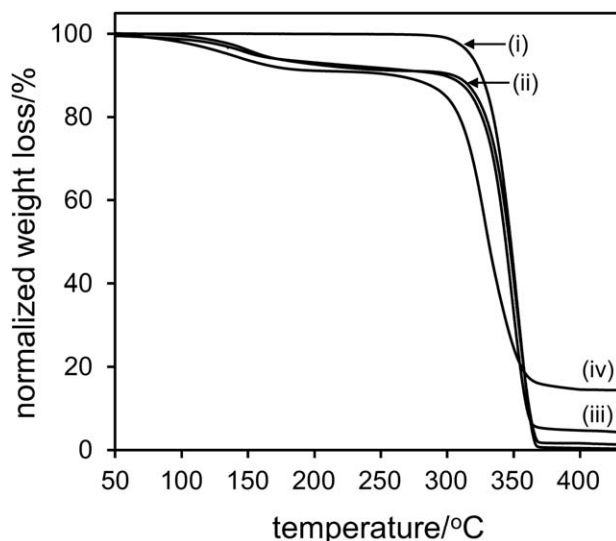


**Figure 4.** Normalized weight loss as a function of temperature for: (i) neat PLA and PLA containing: (ii) 10 wt % thymol, (iii) 10 wt % TK and 10 wt % thymol and (iv) 40 wt % TK and 10 wt % thymol. The thermograms were obtained using a heating rate of 5°C min<sup>-1</sup>.

Figure 7 shows the weight percentage of thymol that remains in the PLA formulation following thermal processing for neat PLA and PLA/TK composites containing different TK loadings where the analyses were conducted using the TG technique and independently confirmed by extraction followed by GC analysis. There is an acceptable level of consistency between the results obtained using the two techniques. The results suggest that the unfilled PLA formulation exhibits the highest level of thymol (*ca.* 8 wt %) following thermal processing and that the ability of the PLA to retain thymol as such decreases upon increased loadings of the TK filler. Generally, during the thermal mixing process, friction occurs between the barrel and screw that may

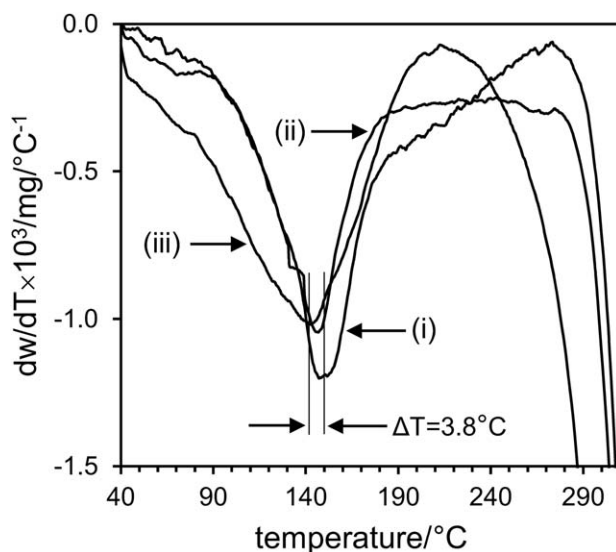


**Figure 5.** Plots of the first derivative with respect to temperature,  $dw/dT$ , of the respective TG weight loss profiles shown in Figure 4 for PLA containing: (i) 10 wt % thymol, (ii) 10 wt % TK and 10 wt % thymol and (iii) 40 wt % TK and 10 wt % thymol.

**Table II.** Thermal Parameters Obtained from the Analyses of the TG Profiles of PLA and PLA/TK Composites Containing Zero, 5% and 10 wt % Thymol.

Thymol content (wt %)	TK content (wt %)	$T_{rel}$ ( $^{\circ}\text{C}^a$ )	$T_{deg}$ ( $^{\circ}\text{C}$ )	%Char residue at 400 $^{\circ}\text{C}$
0	0	-	352.9	0.5
	10	-	346.4	4.2
	40	-	332.5	11.2
5	0	149.9	354.8	1.4
	10	148.2	341.8	5.0
	40	146.8	328.7	12.1
10	0	147.8	352.3	1.7
	10	146.1	348.3	5.2
	40	144.0	328.1	13.2

<sup>a</sup> $T_{rel}$  determinations were performed in triplicate.

lead to the degradation of the AM agents.<sup>40,41</sup> In the current study, it was found that the degradation/release temperature of thymol  $T_{rel}$  in active PLA film (see Table II) was lower (149 $^{\circ}\text{C}$ ) than the processing temperature (155 $^{\circ}\text{C}$ ) at which the melt was mixed for 8–10 min. The latter resulted in a considerable loss of thymol from the PLA formulation containing 10 wt % thymol. A similar finding was observed by Ramos *et al.*<sup>13,20</sup> where *ca.* 75% of the initial thymol remained after processing. Active PLA-based formulations containing butylated hydroxytoluene (BHT) underwent similar losses due to factors such as poor mixing in the extruder, evaporation and thermal degradation of BHT.<sup>42</sup>

The effect of TK loading on the retention of thymol in the formulation can be measured by comparing the residual thymol concentration following processing with the nominal thymol concentration in the formulation. For example, Figure 8 shows

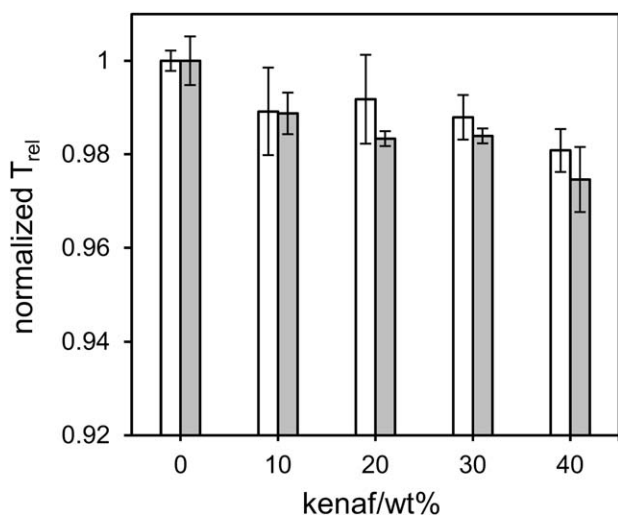


**Figure 6.** Normalized maximum release rate temperature,  $T_{rel}$ , of thymol from PLA and PLA/TK composites containing: 5 wt % (□) and 10 wt % (■) thymol. The determinations were performed in triplicate.

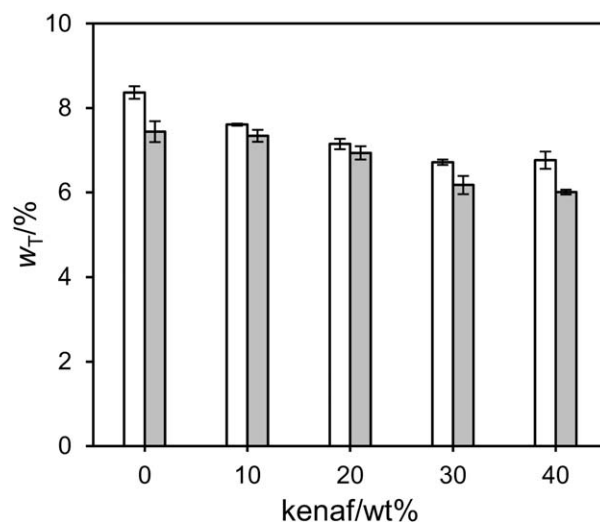


**Figure 7.** Weight percentage of thymol in the PLA formulation following thermal processing as determined using TGA,  $w_T$  for neat PLA and PLA/TK composites containing different kenaf loadings. Analyses were conducted using: TG analysis (□) and extraction/GC (■). The determinations were performed in triplicate.

plots of  $w_T$ , the weight percentage of thymol in the PLA formulation following thermal processing as determined using TG analysis versus  $w_F$ , the nominal weight percentage of thymol in the formulation for systems containing two different TK loadings as well as a plot for a control sample (zero TK loading). The PLA composite containing 10 wt % thymol and the higher TK loading (40 wt %) exhibited lower thymol retention compared to the PLA composite containing 10 wt % thymol and 10 wt % TK loading. However, this effect is not as pronounced at the lower thymol concentration of 5 wt %. Overall, it was found that the final weight percentage of thymol in the PLA/TK composites containing 40 wt % TK could be lower than the nominal weight percentage by up to *ca.* 30%. Furthermore, the

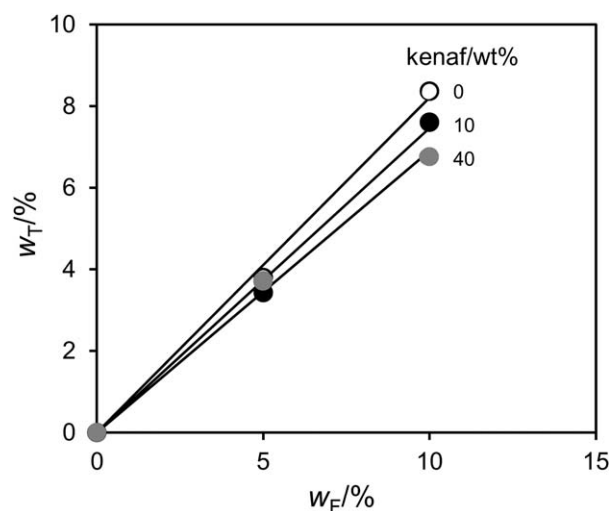


**Figure 8.** Plots of the weight percentage of thymol in the PLA formulation following thermal processing as determined using TGA,  $w_T$ , versus the nominal weight percentage of thymol in the formulation,  $w_F$ , for systems containing: zero (○), 10 wt % (●) and 40 wt % (●) TK loading.

**Table III.** Linear Regression Analyses of PLA and PLA/TK Formulation Containing Zero, 5% and 10 wt % Thymol

Composition	$dwT/dwF$	$r^2$
Neat PLA	0.851	0.993
PLA+10 wt % TK	0.746	0.996
PLA+20 wt % TK	0.724	0.998
PLA+30 wt % TK	0.692	0.990
PLA+40 wt % TK	0.690	0.999

results confirm that as the TK loading is increased, the retention of thymol during processing is decreased.

Analyses similar to those depicted in Figure 8 were conducted at all loadings of TK used in this study and the gradients of the plots,  $dwT/dwF$ , along with the corresponding linear coefficient of determination ( $r^2$ ) are presented in Table III. In all cases the gradient of the neat PLA (control) is greater than the gradient obtained for the composites and there is a concomitant decrease in the gradient with an increase in the TK loading. This confirms that the presence of TK in these latter systems decreases the retention of thymol during processing with retentions ranging from *ca.* 85% (neat PLA) down to *ca.* 69% (40 wt % TK loading) for a thymol concentration of up to 10 wt %.

In the case of PLA/TK composites, the increased loss of thymol at higher TK loadings during processing may be attributable to the higher mechanical shear that exists during the mixing of the composites and that most likely contributes to the loss of thymol from the system through evaporation. The presence of a high content of fiber in the PLA-thymol matrix may also lead to the creation of voids that facilitate the release of thymol from the composite. This suggestion is consistent with the SEM images as seen in Figure 9 where voids and loose fibers are observed on the fracture surface of PLA/kenaf composites containing 10 and 30 wt % thymol. Furthermore, the heat evolved

during the mixing process might liberate moisture in the TK fiber to produce steam and subsequently facilitate the evaporation of thymol. Indeed, the loss of thymol through a process akin to steam distillation is possible as the boiling point of thymol is lowered in the presence of steam. Mulvaney<sup>43</sup> reported that the boiling point of thymol is depressed in the presence of steam, allowing it to evaporate at a temperature below that at which the deterioration of the material becomes appreciable.

### TG Kinetics Analysis

The apparent activation energy ( $E_a$ ) for the release of thymol from both active PLA and PLA/TK composites containing 10, 20 or 30 wt % thymol was calculated by applying a 3D-diffusion model [see eqs. (1) and (3)] based on the TG analysis results (release of thymol,  $T_{rel}$  curve). The results are given in Table IV along with: (i) the corresponding Arrhenius A-factors, (ii) the goodness of fit to the 3D diffusion analysis model as determined on a scale of zero to unity from the computer algorithm, and (iii) the linear regression analyses of the plots of  $g(x)$  versus  $p(x)$ , including the corresponding coefficient of determination,  $r^2$  of the latter. The linearity reflected in the regression analyses demonstrates that the TG fitting protocol is appropriate and provides some degree of confidence in the derived value of the apparent activation energy. Figure 10 shows a typical plot of  $g(x)$  versus  $p(x)$ . In this case the plot pertains to the analysis of the release of thymol from PLA containing 20 wt % TK and 30 wt % thymol. From the gradient of this plot and the Arrhenius A-Factor, the value of  $E_a$  is calculated to be  $68 \text{ kJ mol}^{-1}$  [see eqs. (1) and (2)] and this value corresponds closely to the value of  $65 \text{ kJ mol}^{-1}$  that was delivered by the iterative computer analysis program.

The data listed in Table IV suggest that the apparent activation energy for the release of thymol from PLA is *ca.*  $46 \text{ kJ mol}^{-1}$ . As expected, this value does not appear to depend on the level of thymol and repeated measurements of this parameter for six replicates at three different thymol concentrations in the range

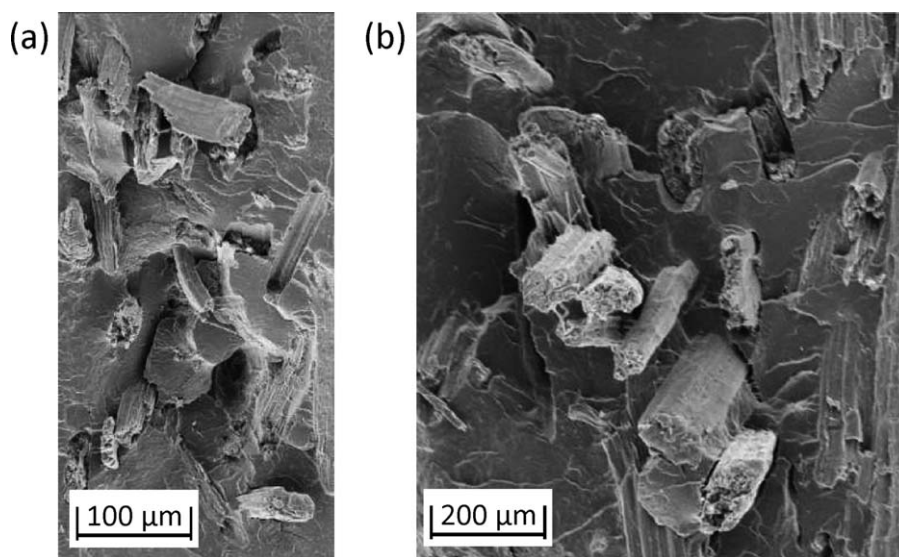


**Figure 9.** Scanning electron micrographs of: (a) PLA/TK composite containing 20 wt % TK and 10 wt % thymol at 100× magnification and (b) PLA/TK composites containing 20 wt % TK and 30 wt % thymol at 200× magnification.

**Table IV.** Kinetics Analyses of TG Data for PLA and PLA/Kenaf Composites Containing Thymol

Formulation	$E_a$ (kJ mol <sup>-1</sup> )	$E_a$ (ave) <sup>a</sup> (kJ mol <sup>-1</sup> )	A (min <sup>-1</sup> )	3D Diff Model Fit	$g(\alpha)$ vs $p(x)$	
					Regression equation	$r^2$
PLA+20Th	46	46 ± 9	6.33E+03	0.922	$y = 8.948E+06x - 2.136E-02$	0.981
PLA+30Th	44		1.50E+03	0.850	$y = 1.647E+06x - 3.666E-03$	0.995
PLA+10Th+30UTK <sup>b</sup>	52	53 ± 6	3.44E+04	0.953	$y = 4.551E+07x - 4.587E-03$	0.988
PLA+10Th+20TK	63		6.26E+05	0.919	$y = 6.202E+08x + 1.991E-02$	0.961
PLA+20Th+20TK	58	65 ± 4	2.72E+05	0.940	$y = 3.864E+08x - 6.240E-03$	0.998
PLA+30Th+20TK	65		1.64E+06	0.905	$y = 2.681E+09x - 4.579E-03$	0.998
PLA+10Th+40TK	69		1.04E+07	0.928	$y = 1.487E+10x + 5.603E-03$	0.997
UK+25Th <sup>b</sup>	96	98 ± 4	1.80E+11	0.960	$y = 4.577E+14x + 1.584E-03$	0.977
TK+25Th <sup>b</sup>	106	105 ± 1	4.32E+12	0.906	$y = 1.583E+16x - 6.636E-03$	0.991

<sup>a</sup> $E_a$  averaged over: six different systems for PLA+thymol; five replicates for PLA+thymol+UK; four different systems for PLA+thymol+TK; three replicates for UK+thymol; two replicates for TK+thymol.

<sup>b</sup>Fibers doped with thymol.

of 10–30 wt % thymol yielded an average result of  $46 \pm 9$  kJ mol<sup>-1</sup>. Similarly, Soto-Valdez *et al.*<sup>44</sup> reported that the apparent activation energy of the diffusion of resveratrol (antioxidant) from PLA films immersed in different food simulants and at different resveratrol concentrations remained almost constant between 175 and 177 kJ mol<sup>-1</sup>. The addition of TK to the formulation significantly increases the apparent  $E_a$  for the release of thymol from the PLA composite matrix, presumably due to the interaction between TK and thymol that was established from the FTIR analysis (see Figure 3 and Table I). Interestingly, it appears that the level of TK does not significantly affect the value of  $E_a$  for thymol release, as there seems only to be a small increase in the latter value when the TK loading is increased from 20 to 40 wt %. Assuming that the  $E_a$  for the release of thymol from these systems is independent of the level of thymol and loading of TK over the respective ranges that were tested in the current study, the  $E_a$  data for the PLA/TK composites containing thymol can be averaged to produce an overall result of  $65 \pm 4$  kJ mol<sup>-1</sup>. Clearly, by comparing this result with the average  $E_a$  value for the release of thymol from PLA alone demonstrates that the addition of TK to the formulation significantly increases the apparent activation energy for the release of thymol. This may be due to the interaction between the thymol and the kenaf as well as the presence of the filler producing a reduction in amorphous regions through which the additive molecules can be released.<sup>44,45</sup>

The interaction between the TK and thymol is also confirmed in the apparent activation energy for the release of thymol from TK fibers doped with 25 wt % thymol. The results in Table IV suggest that the latter  $E_a$  value (106 kJ mol<sup>-1</sup>) is significantly greater than that which is associated with the release of thymol from either the PLA alone or the PLA/thymol/kenaf composites. Whence it can be proposed that the observed increased loss of thymol that occurs on processing TK containing PLA composites (see Figures 6–9) may be due to the presence of the TK which increases friction during processing as well as creates a

more open amorphous structure in the resulting material thereby facilitating the release of the thymol. The data in Table IV are also consistent with the notion that the alkaline chemical pre-treatment of kenaf fibers enhances its compatibility and attractive interactions with substrates such as PLA.<sup>46,47</sup> In the case of its interaction with thymol it can be seen that the apparent  $E_a$  for thymol release from TK (i.e. 106 kJ mol<sup>-1</sup>) is greater than that for its release from UK where the value of the latter is 96 kJ mol<sup>-1</sup>. This difference in thymol release from the doped fibers containing 25 wt % thymol is also reflected in the release of thymol from the corresponding PLA composites. The data in Table IV are consistent in this regard and show that the addition of UK doped with thymol to the PLA composite system lowers as expected the apparent  $E_a$  for the release of thymol from the system.

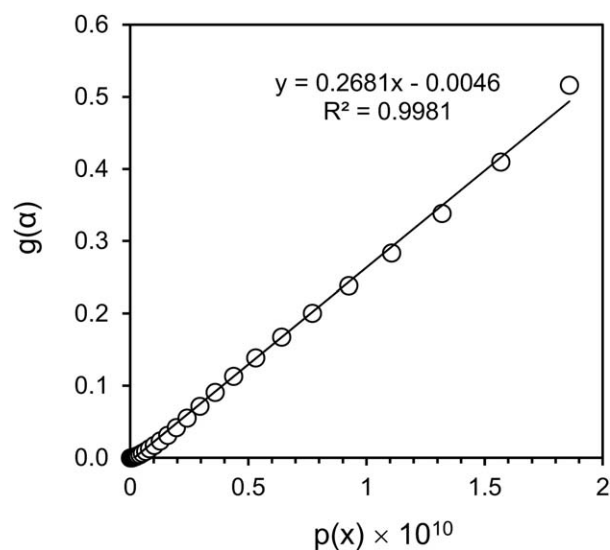


**Figure 10.** A typical plot of  $g(\alpha)$  versus  $p(x)$  for PLA/TK composite containing 20 wt % TK and 30 wt % thymol.

## CONCLUSIONS

The FTIR analysis of the active PLA and PLA/TK composites containing thymol showed that the thymol interacts with PLA and kenaf as revealed by the observed significant shifts in the various FTIR absorption bands. Active PLA/KF composites retain less thymol upon processing than PLA alone and the PLA/KF composites containing the highest fiber loadings demonstrated the lowest retained thymol content. This is despite the fact that the apparent activation energy for thymol release from the PLA/TK composites containing thymol being greater than that found for the release of thymol from PLA alone. It would therefore appear that the disruption to the crystalline regions caused by the addition of kenaf, along with the concomitant creation of voids and the resulting decrease in tortuosity, facilitate the release of the active agent thymol from the composite. These effects seem to overshadow the intermolecular attractions that occur as a result of hydrogen bonding between the components in the composite. Clearly, the interactions between PLA, thymol and kenaf when together in a polymer composite are complex and it is difficult to make any further generalizations based on the data obtained so far. Nonetheless, the exploration of the interactions that exist between the pairs of separate components in these systems can give valuable insight into the mechanism of AM loss during processing and assist in identifying measures that will minimize such losses in future commercial applications.

## ACKNOWLEDGMENTS

The authors gratefully acknowledge the Ministry of Education, Malaysia and the Universiti Putra Malaysia (UPM) for providing the PhD scholarship for Intan Tawakkal and acknowledge the assistance of technical staff from RMIT University especially Mr. Mike Allan for the preparation of the composite samples.

## REFERENCES

- Lo Re, G.; Morreale, M.; Scaffaro, R.; La Mantia, F. P. *Polym. Int.* **2012**, *61*, 1542.
- Valdés, A.; Mellinas, A. C.; Ramos, M.; Garrigós, M. C.; Jiménez, A. *Polym. Chem.* **2014**, *2*, 1.
- Li, W. L.; Coffin, D. R.; Jin, T. Z.; Latona, N.; Liu, C. K.; Liu, B.; Zhang, J.; Liu, L. S. *J. Appl. Polym. Sci.* **2012**, *126*, 361.
- Kijchavengkul, T.; Auras, R. *Polym. Int.* **2008**, *57*, 793.
- González, A.; Igarzabal, C. I. A. *Food Hydrocoll.* **2013**, *33*, 289.
- Jin, T.; Zhang, H. *J. Food Sci.* **2008**, *73*, 127.
- Tawakkal, I. S. M. A.; Cran, M. J.; Bigger, S. W. *Ind. Crop. Prod.* **2014**, *61*, 74.
- Kumar, R.; Münstedt, H. *Polym. Int.* **2005**, *54*, 1180.
- Martínez-Camacho, A. P.; Cortez-Rocha, M. O.; Castillo-Ortega, M. M.; Burgos-Hernández, A.; Ezquerro-Brauer, J. M.; Plascencia-Jatomea, M. *Polym. Int.* **2011**, *60*, 1663.
- Bonilla, J.; Fortunati, E.; Vargas, M.; Chiralt, A.; Kenny, J. M. *J. Food Eng.* **2013**, *119*, 236.
- Del Nobile, M. A.; Conte, A.; Buonocore, G. G.; Incoronato, A. L.; Massaro, A.; Panza, O. *J. Food Eng.* **2009**, *93*, 1.
- Han, J. H. In *Novel Food Packaging Techniques*; R. Ahvenainen, Ed.; Woodhead Publishing Ltd., Cambridge, **2003**, p 50.
- Ramos, M.; Jiménez, A.; Peltzer, M.; Garrigós, M. C. *J. Food Eng.* **2012**, *109*, 513.
- Wu, Y.; Yuan, M. W.; Yang, J. Y.; Qin, Y. Y.; Yuan, M. L.; Cao, J. X. *Adv. Mater. Res.* **2014**, *884*, 481.
- Guarda, A.; Rubilar, J. F.; Galotto, M. J.; Universidad de Santiago de Chile: Chile, **2012**, p 43.
- Tunç, S.; Duman, O. *LWT-Food Sci. Technol.* **2011**, *44*, 465.
- Tao, F.; Hill, L. E.; Peng, Y.; Gomes, C. L. *LWT-Food Sci. Technol.* **2014**, *59*, 247.
- Nyambo, C.; Mohanty, A. K.; Misra, M. *Macromol. Mater. Eng.* **2011**, *296*, 710.
- Suppakul, P.; Victoria University of Technology: Melbourne **2004**, p 259.
- Ramos, M.; Jiménez, A.; Peltzer, M.; Garrigós, M. C. *Food Chem.* **2014**, *162*, 149.
- Liu, L. S.; Jin, T. Z.; Coffin, D. R.; Hicks, K. B. *J. Agric. Food Chem.* **2009**, *57*, 8392.
- Praprudivongs, C.; Sombatsompop, N. *Compos.: Part B* **2012**, *43*, 2730.
- Woraprayote, W.; Kingcha, Y.; Amonphanpokin, P.; Krueate, J.; Zendo, T.; Sonomoto, K.; Benjakul, S.; Visessanguan, W. *Int. J. Food Microbiol.* **2013**, *167*, 229.
- Akil, H. M.; Omar, M. F.; Mazuki, A. A. M.; Safiee, S.; Ishak, Z. A. M.; Abu Bakar, A. *Mater. Des.* **2011**, *32*, 4107.
- Saba, N.; Paridah, M. T.; Jawaid, M. *Construct. Build. Mater.* **2015**, *76*, 87.
- Shukor, F.; Hassan, A.; Saiful Islam, M.; Mokhtar, M.; Hasan, M. *Mater. Des.* **2014**, *54*, 425.
- Flynn, J. H. In *Thermal Analysis Volume 2: Inorganic Materials and Physical Chemistry*; Schwenkerand, R. F., Garn, P. D. Eds.; Elsevier Science: Burlington, **1969**; p 1111.
- Brown, M. E. *Introduction to Thermal Analysis: Vol. 1 Techniques and Applications*, Springer: New York, **2001**.
- Dollimore, D.; Evans, T. A.; Lee, Y. F.; Pee, G. P.; Wilburn, F. W. *Thermochim. Acta* **1992**, *196*, 255.
- Wang, D. K.; Varanasi, S.; Fredericks, P. M.; Hill, D. J. T.; Symons, A. L.; Whittaker, A. K.; Rasoul, F. *J. Polym. Sci. Part A* **2013**, *51*, 5163.
- Goncalves, C. M. B.; Coutinho, J. A. P.; Marrucho, I. M.; In Poly(lactic acid): Synthesis, Structures, Properties, Processing and Applications; Auras, R. A.; Lim, L. T.; Selkeand, S. E. M.; Tsuji, H., Eds.; Wiley: Chichester, **2011**; p 97.
- Al-Sheibany, I. S.; Kadhim, K. H.; Abdullah, A. S. *Natl. J. Chem.* **2005**, *19*, 366.
- Sun, Y.; Cheng, J. *Bioresour. Technol.* **2002**, *83*, 1.
- Himmelsbach, D. S.; Khalili, S.; Akin, D. E. *J. Sci. Food Agric.* **2002**, *82*, 685.
- Bax, B.; Müssig, J. *Compos. Sci. Technol.* **2008**, *68*, 1601.
- Garlotta, D. *J. Polym. Environ.* **2001**, *9*, 63.

37. Ramos, M.; Fortunati, E.; Peltzer, M.; Dominici, F.; Jiménez, A.; Garrigós, M. D. C.; Kenny, J. M. *Polym. Degrad. Stab.* **2014**, *108*, 158.
38. Yussuf, A. A.; Massoumi, I.; Hassan, A. *J. Polym. Environ.* **2010**, *18*, 422.
39. Persico, P.; Ambrogi, V.; Carfagna, C.; Cerruti, P.; Ferrocino, I.; Mauriello, G. *Polym. Eng. Sci.* **2009**, *49*, 1447.
40. Soto-Cantú, C. D.; Graciano-Verdugo, A. Z.; Peralta, E.; Islas-Rubio, A. R.; González-Córdova, A.; González-León, A.; Soto-Valdez, H. *J. Dairy Sci.* **2008**, *91*, 11.
41. Graciano-Verdugo, A. Z.; Soto-Valdez, H.; Peralta, E.; Cruz-Zárate, P.; Islas-Rubio, A. R.; Sánchez-Valdes, S.; Sánchez-Escalante, A.; González-Méndez, N.; González-Ríos, H. *Food Res. Int.* **2010**, *43*, 1073.
42. Ortiz-Vazquez, H.; Shin, J.; Soto-Valdez, H.; Auras, R. *Polym. Test.* **2011**, *30*, 463.
43. Mulvaney, J. *Aus. J. Herb. Med.* **2012**, *24*, 140.
44. Soto-Valdez, H.; Auras, R.; Peralta, E. *J. Appl. Polym. Sci.* **2011**, *121*, 970.
45. Limm, W.; Hollifield, H. C. *Food Add. Contam.* **1996**, *13*, 949.
46. Huda, M. S.; Drzal, L. T.; Mohanty, A. K.; Misra, M. *Compos. Sci. Technol.* **2008**, *68*, 424.
47. Ibrahim, N. A.; Yunus, W. M. Z. W.; Othman, M.; Abdan, K. *J. Reinf. Plast. Compos.* **2011**, *30*, 381.